Veto Cut Efficiency Analysis. (PrimEx Note)

To extract cross sections with veto cut, one needs to know its efficiency. We used data from the second snake scan to extract it. prim_ana package was used in the analysis.

A veto counter response was determined by signals from both, top and bottom veto PMT. A time interval between the signals should be:

$|t_1 - t_2| < 25$ ns,

$|(t_1 + t_2)/2 - t_{HyCal}| < 15$ ns,

where t_1, t_2 - time from VETO PMTs, t_{HyCal} - time from HyCal total sum.

There are several types of Veto to HyCal matching in analysis: reconstructed X of the HyCal cluster with Veto counter X match; reconstructed y of a cluster with Y reconstructed by Veto match; time difference between Veto and Hycal events. To determine veto response in further analysis any of type of matching (listed above) were used.

Fig. 1 shows probability to match neutral particle as a charged by Veto counters for these matching types. One run used for this figure is a scan of a single row of the lead glass top panel, the second run is a scan of a single row of the crystal region.

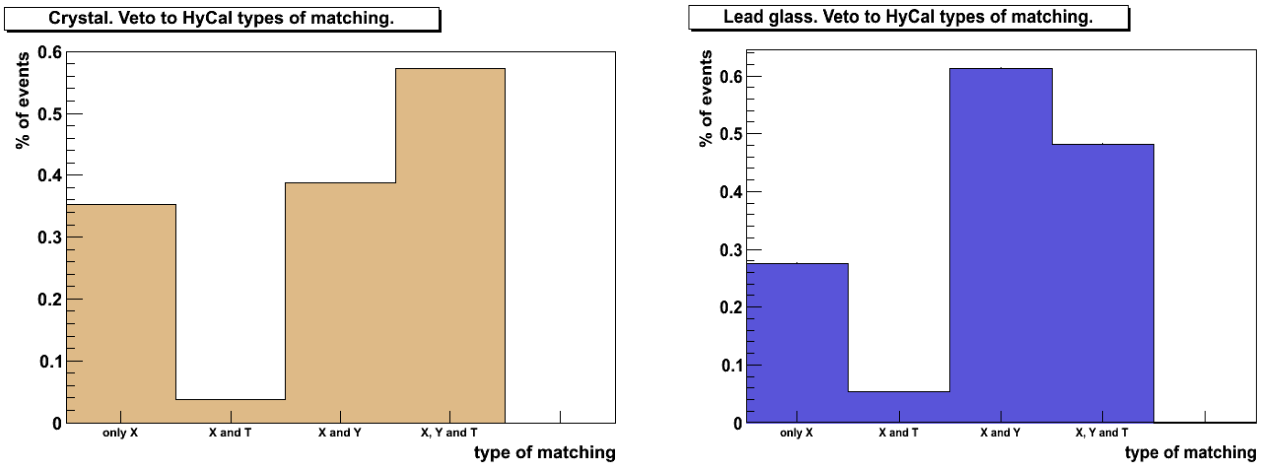

Fig.1 (a,b) Veto response (% of events) versus HyCal types of matching.
1st bin - match only by X coordinate.
2nd bin - match by X and time.
3rd bin - match by X and Y coordinates only.
4th bin - match by all: X, Y and time.
Plot (a) is for crystal region. Plot (b) - for lead glass region.

Information from clock trigger events was analyzed to estimate a rate of veto response accidentals. 140K clock trigger events from second snake run were analyzed. An estimated rate of accidental veto response is negligible (less than 0.01% of events).

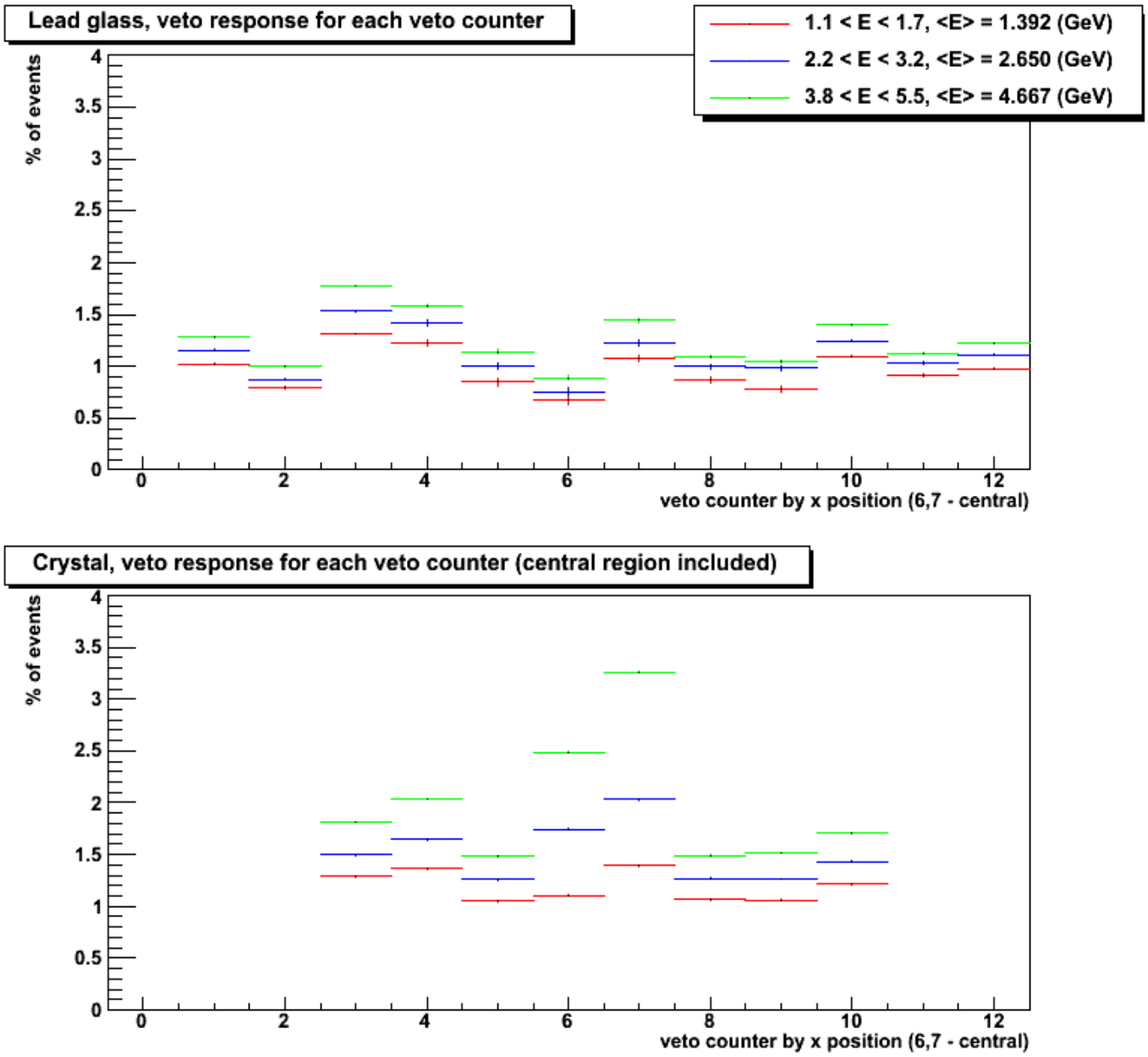

Fig. 2(a,b). Probabilities to match a neutral particle as a charged for each veto counter for different energy ranges.
Plot (a) - for lead glass region, plot (b) - for crystal region.

Fig. 2 shows the probabilities to match a neutral particle as a charged for each veto counter for different energy ranges. The analysis uses all snake-2 statistics. One can see that the probability to match a neutral particle as a charged increases with higher energy for both plots. Also there is a a significant higher veto response for two central (6, 7 on the figure) veto counters for high energies on Fig. 4. Such a high veto response is described by a leakage from longitudinal sides if tungsten shield.

To estimate a tungsten shield influence Fig 3 (a,b) was plotted. Fig. 3(a) shows a veto response for all crystal region except for the central square of 6x6 HyCal modules. Fig 3(b) shows a veto response for the central square of 6x6 HyCal modules only.

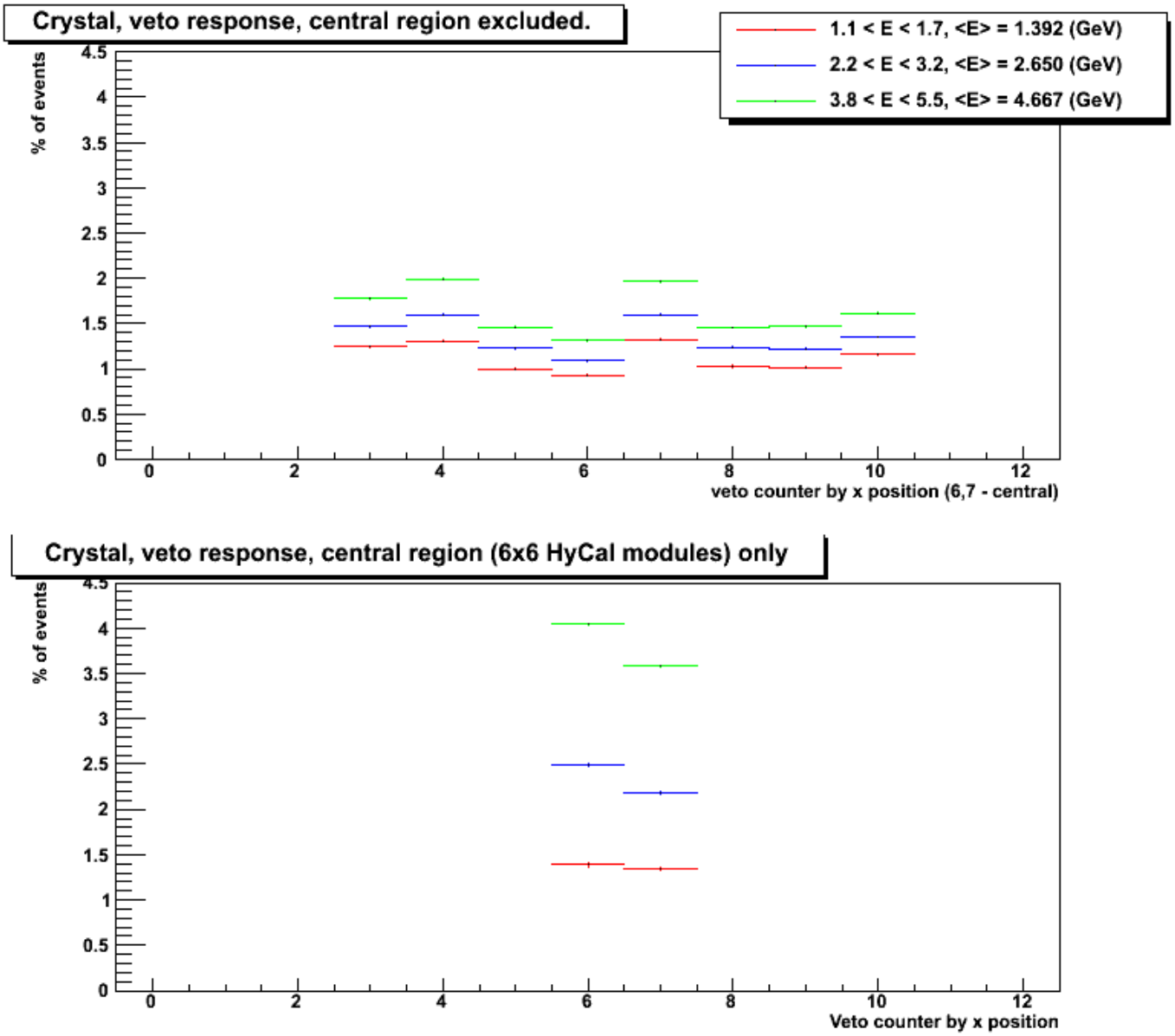

Fig. 3(a,b). Probabilities to match a neutral particle as a charged for each veto counter for different energy ranges.
Plot (a) - all crystal region excluding the central square of 6x6. Plot (b) for the central square of 6x6 HyCal modules.

To estimate an energy dependence, a veto response versus energy by tagger and by HyCal was plotted.

Fig. 4 (a,b) shows an energy by tagger, and veto response versus this energy. The figures illustrate a linear energy dependence.

Fig. 5(a,b) shows HyCal energy, and veto response versus this energy. One can see a significant increase of veto response for energy regions that is absent in tagger energy range. Such an increasing is possibly described by Compton effect on material in gamma quantum way.

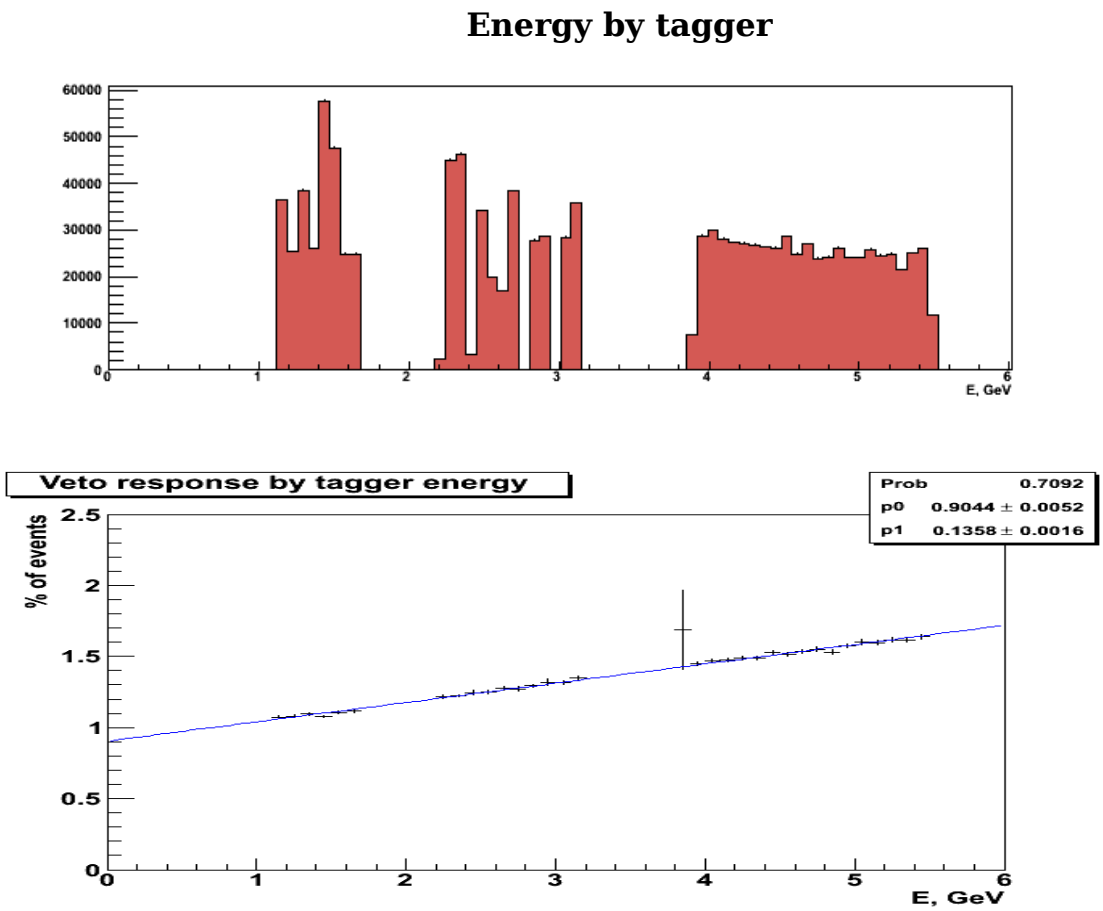

Fig. 4. Plot (a) - Energy by Tagger. Plot (b) - veto response versus energy by Tagger.

Energy by HyCal

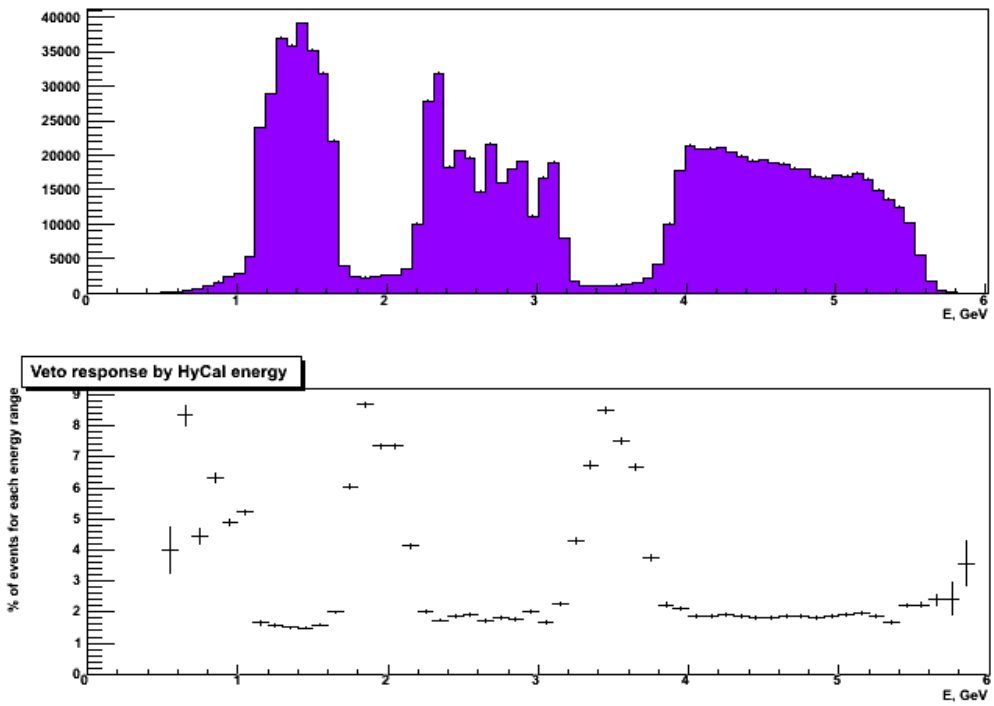

Fig. 5. Plot (a) - Energy by HyCal. Plot (b) - veto response versus energy by HyCal.

To reduce this effect following cuts was applied:
$|E_{hycal}/E_{tagger} - 1| < 0.09$ (for crystals)
$|E_{hycal}/E_{tagger} - 1| < 0.14$ (for lead glass)
(Both values corresponds to 3*sigmas in elasticity distribution.)

Trig photon tdif: between -5 and +15 ns

$|X - X_{mean}| < 1cm$
$|Y - Y_{mean}| < 1cm$

Where X and Y are current HyCal cluster reconstructed coordinates; X_{mean}, Y_{mean} are the mean values for the last 1000 reconstructed coordinates.

A veto response versus energy by HyCal after applying of this cuts is shown on fig. 6.

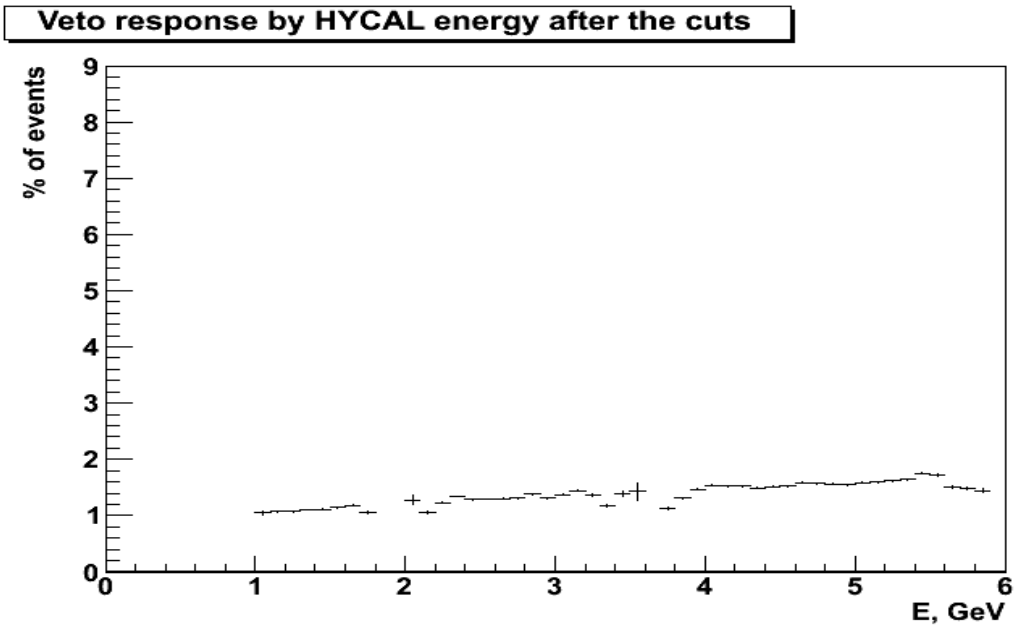

Fig. 6. Veto response versus energy by HyCal after the cuts.

Fig. 7 shows the veto response versus an energy by tagger dependence for different regions of HyCal. All the distributions has a linear dependence and was fitted by first order polynom.

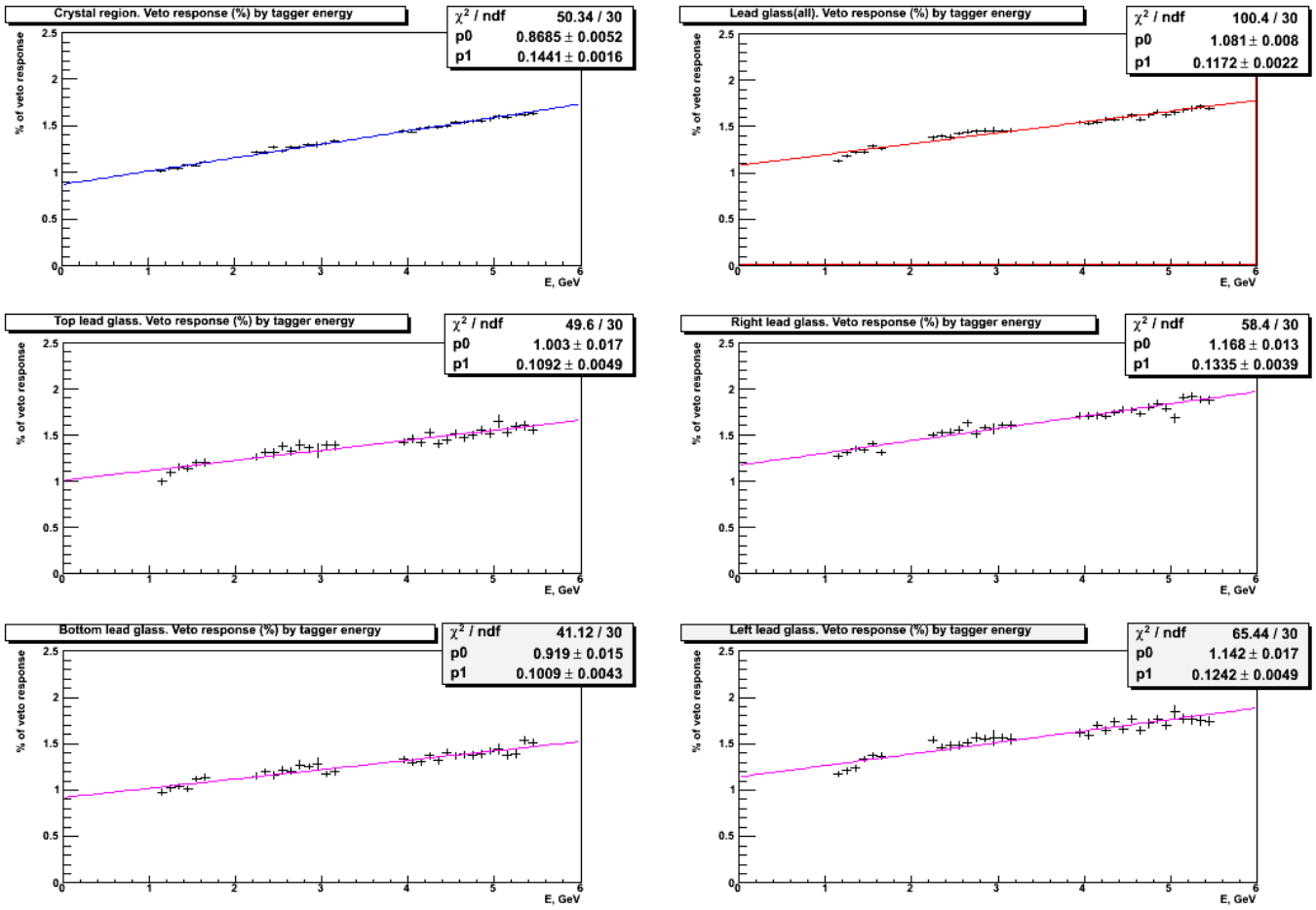

Fig. 7. Veto response versus an energy by tagger dependence for different regions of HyCal.

To use this results in a further analysis a table of veto response for each HyCal module for 3 energy ranges is obtained. Fig. 8(a) shows veto responses for each HyCal module for 1.1<E (GeV)<1.7 energy and Fig. 8(b) is for 3.8<E (GeV)<5.5 energy. One can see the vertical structure of distribution that corresponds to veto plates and an increase of veto response probability for the crystal-lead glass transition area. There is also a lack of veto response for the top and bottom glass regions near the edges of the HyCal. This is possibly described by less probability for signal to reach an opposite side PMT.

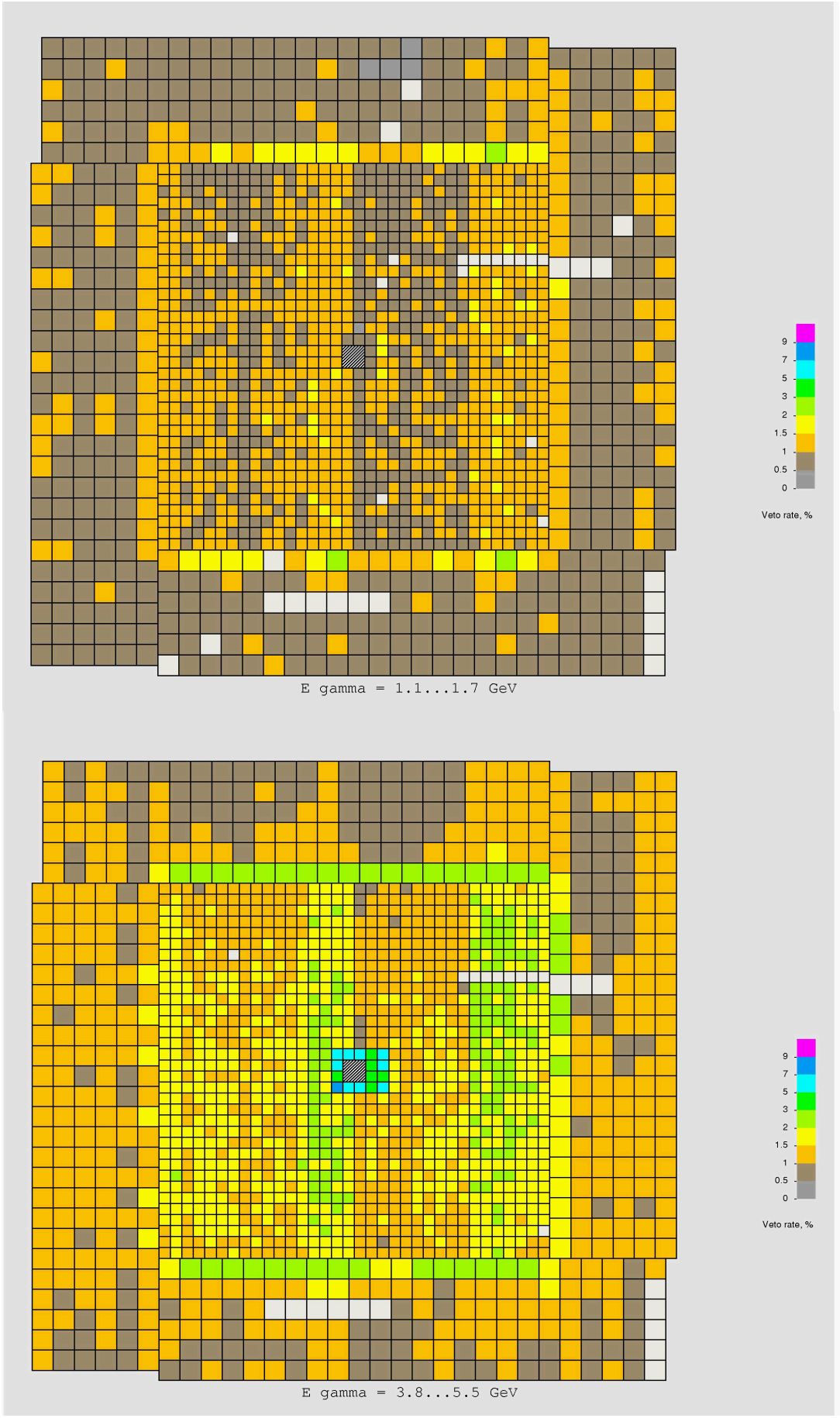

Fig. 8 veto responses for each HyCal module. Plot (a) is for 1.1< E (GeV) <1.7 energy and Plot (b) is for 3.8< E (GeV) <5.5 energy.